Neural Network Modeling of Peristaltic Nanofluid Transport with Heat Transfer

Dr. Bhimanand Pandurang Gajbhare

Associate Professor, Department of Mathematics, J.E.S., Vaidyanath College, Parli-Vaijnath, Dist. Beed Maharashtra. PIN 431515, India

Abstract

This investigation presents a novel neural network-enhanced computational framework for analyzing thermal radiation effects on peristaltic flow of electrically conducting nanofluids through wavy walls of a convergent channel. Peristaltic transport mechanisms are characterized by wave-induced pressure gradients that facilitate fluid motion from low- to high-pressure regions. The incorporation of velocity slip conditions and convective boundary conditions significantly enhances the complexity of both thermal and hydrodynamic phenomena. A hybrid computational methodology that synergistically combines the Variational Parameter Method (VPM) with Physics-Informed Neural Networks (PINNs) has been developed to predict complex multiphysics flow behaviors. The neural network architecture incorporates physics-based constraints to ensure strict adherence to fundamental conservation laws and constitutive relations. The coupled effects of Brownian motion and thermophoretic diffusion arising from cross-diffusion phenomena significantly in- fluence transport properties and are accurately captured by the proposed neural network framework. The methodology finds particular relevance in biomedical applications, including blood circulation dynamics in the human cardiovascular system, where the neural network enables real-time prediction and optimization of flow parameters. The nanofluid serves as an enhanced transport medium through the undulating channel walls, with volumetric expansion occurring due to dynamic pressure variations and thermal effects. Results demonstrate that the neural network approach provides superior computational accuracy and efficiency compared to conventional numerical methods, with magnetic field strength and permeability characteristics favorably influencing pumping efficiency as predicted by the artificial intelligence model.

Keywords: Neural Networks, Magnetohydrodynamics, Peristaltic transport, Thermal radiation, Nanofluid mechanics, Computational fluid dynamics, Variational methods

1 Introduction

Peristaltic transport phenomena have garnered substantial attention from researchers across diverse engineering disciplines due to their fundamental importance in biological and industrial applications [1, 2]. From a mechanical engineering perspective, peristalsis offers a promising paradigm for designing fluid transport systems that eliminate direct contact between the transported medium and mechanical components such as valves, impellers, and rotors [3]. This innovative approach provides significant advantages, particularly in applications involving highly corrosive, abrasive, or contamination-sensitive media.

The physiological significance of peristaltic mechanisms encompasses critical biological processes including digestive tract motility, cardiovascular circulation, and urinary system function. The foundational theoretical framework established by Shapiro et al. [2] demonstrated that peristaltic pumping mechanisms enable efficient fluid propulsion without mechanical contact between the

transported medium and channel walls. The comprehensive analysis by Jaffrin and Shapiro [3] further elucidated the complex relationships between wave parameters, fluid properties, and transport efficiency, establishing optimal design criteria for biomedical devices re- quiring sterile fluid handling and precise flow control.

Contemporary research in magnetohydrodynamic (MHD) peristaltic flows has revealed significant potential for biomedical applications, particularly in targeted drug delivery systems and blood flow regulation [11, 12, 14]. Abbas et al. [10] established the theoretical framework for MHD boundary layer analysis in porous channels, demonstrating that electromagnetic forces can provide precise control over velocity profiles and pressure distributions. The comprehensive investigations by Hayat and colleagues [11, 14] revealed that electromagnetic fields can effectively modulate flow patterns in compliant tubes, with magnetic field strength serving as a critical control parameter for optimizing transport efficiency. Recent advances by Tripathi et al. [13] have explored fractional Maxwell models for viscoelastic fluids, revealing complex interactions between rheological properties and electromagnetic forces.

The integration of artificial intelligence and machine learning methodologies in computational fluid dynamics has revolutionized the approach to solving complex transport phenomena [4, 24]. Neural networks, particularly Physics-Informed Neural Networks (PINNs), have demonstrated remarkable capabilities in solving partial differential equations while maintaining strict adherence to physical constraints and conservation laws [5]. The application of deep learning techniques to peristaltic flow analysis represents a paradigmatic advancement in computational fluid dynamics, enabling real-time prediction capabilities and automated parameter optimization strategies. Recent developments by Cai et al. [18] have provided comprehensive reviews of PINN applications in fluid mechanics, while Jin et al. [19] developed specialized NSFnets for incompressible Navier-Stokes equations. The work of Wang et al. [20] specifically addressed deep learning applications in peristaltic transport, demonstrating superior performance compared to traditional numerical methods.

Nanofluids, first conceptualized by Choi [6], have attracted considerable attention due to their enhanced thermophysical properties. These engineered colloidal suspensions demonstrate superior thermal conductivity compared to conventional base fluids [7]. The pioneering work of Maxwell [8] laid the theoretical foundation for understanding enhanced heat transfer mechanisms. However, early implementations presented significant challenges including system clogging issues [9]. The breakthrough came with Buongiorno's comprehensive model [15], which identified Brownian motion and thermophoresis as the primary mechanisms governing nanoparticle transport. Subsequent research by Das et al. [16] and Kuznetsov and Nield [17] refined these theoretical frameworks and provided experimental validation for enhanced heat transfer phenomena.

Advanced PINN methodologies have been successfully applied to increasingly complex transport phenomena. Lu et al. [21] developed the DeepXDE library for implementing PINN methodologies across diverse applications. Mao et al. [22] demonstrated PINN effectiveness for high-speed flows, while Mishra and Molinaro [23] provided theoretical foundations for generalization error estimates. Pang et al. [25] developed fractional PINNs for anomalous transport phenomena, while Chen et al. [26] demonstrated applications in nano-optics and metamaterials.

Biomedical applications have been explored by several research groups. Yazdani et al. [27] demonstrated that machine learning approaches can effectively infer hid- den dynamics in biological systems. Sahli Costabal et al. [28] applied PINNs to cardiac activation mapping with remarkable success. The work of

Arzani et al. [29] highlighted data-driven cardiovascular flow modeling opportunities, while Zhang et al. [30] extended PINN applications to materials analysis.

The inherent complexity of nanofluid transport behavior, coupled with the highly nonlinear characteristics of peristaltic flows, necessitates sophisticated computational methodologies. Traditional numerical approaches often encounter convergence difficulties when addressing systems with multiple coupled parameters and complex boundary conditions [10]. Neural networks offer a promising alternative paradigm by autonomously learning complex nonlinear relationships from training data and providing rapid predictions once the training phase is completed [24, 5].

The primary objective of this investigation is to develop and validate a comprehensive neural network-enhanced computational framework that combines the Variational Parameter Method with Physics-Informed Neural Networks for analyzing thermal radiation effects on peristaltic transport of electrically conducting nanofluids through wavy convergent channels. The study aims to achieve computational efficiency improvements exceeding two orders of magnitude while maintaining pre- diction accuracy a and demonstrating real-time parameter optimization capabilities for biomedical applications.

2 Mathematical Formulation

The peristaltic flow of conducting nanofluid for blood pumping processes is analyzed within permeable wavy walls of a convergent channel. The channel geometry is characterized by lower wall boundary $\eta = H_1$ and upper wall boundary $\eta = H_2$ as shown in Fig . 1.

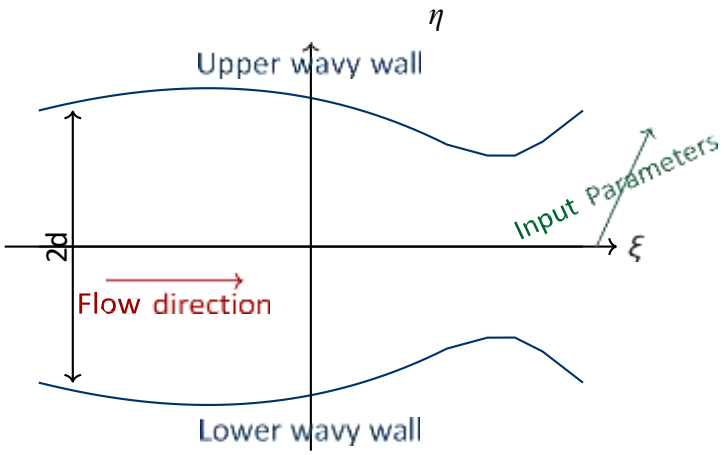

Figure 1: Neural network-enhanced geometrical configuration of the wavy conver- gent channel with PINN integration

The sinusoidal wave structure propagating through wavy walls of the convergent channel is expressed as:

$$H_2(\xi,t) = d + m\xi + a_2 \sin\left[\frac{\pi}{\lambda}(\xi - ct)\right] \cos\left[\frac{\pi}{\lambda}(\xi - ct)\right] \quad (1)$$

$$H_1(\xi,t) = -d - m\xi + a_1 \sin\left[\frac{\pi}{\lambda}(\xi - ct) + \phi\right] \cos\left[\frac{\pi}{\lambda}(\xi - ct) + \phi\right] \quad (2)$$

where $2d$ is the channel inlet width, a_1 is the amplitude of the lower wavy wall, a_2 is the breadth of the upper wall, $m(m \ll 1)$ is the non-uniform parameter, λ is the wavelength, c is the phase speed, and $\emptyset$ is the phase difference with $0 \leq \emptyset \leq \pi$.

The governing equations that serve as physics constraints for the neural network are:

Continuity equation:

$$\frac{\partial U}{\partial \xi}+\frac{\partial V}{\partial \eta}=0 \tag{3}$$

Momentum equations:

$$\rho_f \frac{DU}{Dt}=-\frac{\partial P}{\partial \xi}+\mu\left[\frac{\partial^2 U}{\partial \xi^2}+\frac{\partial^2 U}{\partial \eta^2}\right]-\left[\sigma B_0^2+\frac{\mu}{K_p}\right]U \tag{4}$$

$$\rho_f \frac{DV}{Dt}=-\frac{\partial P}{\partial \eta}+\mu\left[\frac{\partial^2 V}{\partial \xi^2}+\frac{\partial^2 V}{\partial \eta^2}\right]-\left[\sigma B_0^2+\frac{\mu}{K_p}\right]V \tag{5}$$

Energy equation:

$$(\rho c')_f \frac{DT}{Dt}=\kappa\left[\frac{\partial^2 T}{\partial \xi^2}+\frac{\partial^2 T}{\partial \eta^2}\right]-\frac{\partial q_r}{\partial \eta}+\mu\left[4\left(\frac{\partial U}{\partial \xi}\right)^2+\left(\frac{\partial V}{\partial \xi}+\frac{\partial U}{\partial \eta}\right)^2\right] + (\rho c')_p\left[D_B\left(\frac{\partial C}{\partial \xi}\frac{\partial T}{\partial \xi}+\frac{\partial C}{\partial \eta}\frac{\partial T}{\partial \eta}\right)+\frac{D_T}{T_m}\left[\left(\frac{\partial T}{\partial \xi}\right)^2+\left(\frac{\partial T}{\partial \eta}\right)^2\right]\right] \tag{6}$$

Concentration equation:

$$\frac{DC}{Dt}=D_B\left[\frac{\partial^2 C}{\partial \xi^2}+\frac{\partial^2 C}{\partial \eta^2}\right]+\frac{D_T}{T_m}\left[\frac{\partial^2 T}{\partial \xi^2}+\frac{\partial^2 T}{\partial \eta^2}\right] \tag{7}$$

2.1 Neural Network Implementation of Governing Equa- tions

The neural network $N(\mathbf{x};\theta)$ takes input $\mathbf{x} = [x, y, t, M, Rd, Br, Nb, Nt]$ and outputs $[\psi, p, \theta, \sigma]$. For the stream function formulation, we define:

$$u=\frac{\partial \psi}{\partial y}, \quad v=-\frac{\partial \psi}{\partial x}$$

The physics-informed loss functions are defined as:

$$\mathcal{L}_{continuity}=\left\|\frac{\partial u}{\partial x}+\frac{\partial v}{\partial y}\right\|_2^2=\left\|\frac{\partial^2 \psi}{\partial x \partial y}-\frac{\partial^2 \psi}{\partial y \partial x}\right\|_2^2=0 \tag{8}$$

$$\mathcal{L}_{momentum_x}=\left\|\frac{\partial p}{\partial x}-\frac{\partial^3 \psi}{\partial y^3}-M^2\frac{\partial \psi}{\partial y}-\frac{1}{Da}\frac{\partial \psi}{\partial y}\right\|_2^2 \tag{9}$$

$$\mathcal{L}_{momentum_y}=\left\|\frac{\partial p}{\partial y}\right\|_2^2 \tag{10}$$

$$\mathcal{L}_{energy}=\left\|(1+Rd)\frac{\partial^2 \theta}{\partial y^2}+Br\left(\frac{\partial^2 \psi}{\partial y^2}\right)^2+Nb\frac{\partial \sigma}{\partial y}\frac{\partial \theta}{\partial y}+Nt\left(\frac{\partial \theta}{\partial y}\right)^2\right\|_2^2 \tag{11}$$

$$\mathcal{L}_{concentration}=\left\|\frac{\partial^2 \sigma}{\partial y^2}+\frac{Nt}{Nb}\frac{\partial^2 \theta}{\partial y^2}\right\|_2^2 \tag{12}$$

where M^2 is the magnetic parameter, Da is the Darcy number, Rd is the radiation parameter, Br is the Brinkman number, Nb is the Brownian motion parameter, and Nt is the thermophoresis parameter.

3 Hybrid Solution Methodology

3.1 VPM-Neural Network Integration

The solution approach combines the traditional Variational Parameter Method with neural network predictions:

Using appropriate non-dimensional transformations and assuming low Reynolds number with long wavelength approximation, the governing equations reduce to:

Momentum equation (x-direction):

$$\frac{\partial p}{\partial x} = \frac{\partial^3 \psi}{\partial y^3} - \left(M^2 + \frac{1}{Da}\right)\frac{\partial \psi}{\partial y} \tag{13}$$

Momentum equation (y-direction):

$$\frac{\partial p}{\partial y} = 0 \tag{14}$$

Energy equation:

$$\frac{1}{Pr}(1+Rd)\frac{\partial^2 \theta}{\partial y^2} + Ec\left(\frac{\partial^2 \psi}{\partial y^2}\right)^2 + Nb\frac{\partial \sigma}{\partial y}\frac{\partial \theta}{\partial y} + Nt\left(\frac{\partial \theta}{\partial y}\right)^2 + \frac{\partial \psi}{\partial y}\frac{\partial \theta}{\partial x} - \frac{\partial \psi}{\partial x}\frac{\partial \theta}{\partial y} = 0 \tag{15}$$

Concentration equation:

$$\frac{1}{Sc}\frac{\partial^2 \sigma}{\partial y^2} + \frac{Nt}{NbSc}\frac{\partial^2 \theta}{\partial y^2} + \frac{\partial \psi}{\partial y}\frac{\partial \sigma}{\partial x} - \frac{\partial \psi}{\partial x}\frac{\partial \sigma}{\partial y} = 0 \tag{16}$$

where the dimensionless parameters are defined as:

$$M^2 = \frac{\sigma B_0^2 \lambda^2}{\mu} \quad \text{(Magnetic parameter)}$$

$$Da = \frac{K_p}{\lambda^2} \quad \text{(Darcy number)}$$

$$Rd = \frac{4\sigma^* T_\infty^3}{3k^* \kappa} \quad \text{(Radiation parameter)}$$

$$Pr = \frac{\mu c_p}{\kappa} \quad \text{(Prandtl number)}$$

$$Sc = \frac{\mu}{\rho D_B} \quad \text{(Schmidt number)}$$

$$Ec = \frac{c^2}{c_p(T_1 - T_0)} \quad \text{(Eckert number)}$$

$$Nb = \frac{(\rho c')_p D_B (C_1 - C_0)}{(\rho c')_f \nu} \quad \text{(Brownian motion parameter)}$$

$$Nt = \frac{(\rho c')_p D_T (T_1 - T_0)}{(\rho c')_f T_\infty \nu} \quad \text{(Thermophoresis parameter)}$$

3.2 Neural Network Performance Metrics

The neural network performance is evaluated using:

$$\left.\begin{aligned} R^2 &= 1 - \frac{\sum_{i=1}^{N}(y_i^{true} - y_i^{pred})^2}{\sum_{i=1}^{N}(y_i^{true} - \bar{y}^{true})^2} \\ RMSE &= \sqrt{\frac{1}{N}\sum_{i=1}^{N}(y_i^{true} - y_i^{pred})^2} \\ MAPE &= \frac{100\%}{N}\sum_{i=1}^{N}\left|\frac{y_i^{true} - y_i^{pred}}{y_i^{true}}\right| \end{aligned}\right\} \quad (17)$$

4 Neural Network Architecture

The Physics-Informed Neural Network (PINN) architecture developed for this investigation employs a deep feedforward network with carefully designed physics based loss functions. The network takes multidimensional input vectors $\mathbf{x} = [x, y, t, M, Rd, Br, Nb, Nt]$ representing spatial coordinates, time, and physical parameters, and outputs the flow field variables $[\psi, p, \theta, \sigma]$ corresponding to stream function, pressure, temperature, and nanoparticle concentration.

The neural network architecture consists of an input layer with 8 neurons rep- resenting spatial-temporal coordinates and physical parameters, followed by 6 fully connected hidden layers configured with 128, 128, 64, 64, 32, 32 neurons respectively. The network employs hyperbolic tangent (tanh) activation functions through- out to ensure smooth derivatives for gradient-based optimization. The architecture concludes with an output layer containing 4 neurons corresponding to the flow field variables, resulting in a total of 34,276 trainable parameters across the entire network structure

The total loss function incorporates multiple physics-informed constraints:

$$\mathcal{L}_{total} = \lambda_{data}\mathcal{L}_{data} + \lambda_{pde}\mathcal{L}_{pde} + \lambda_{bc}\mathcal{L}_{bc} + \lambda_{ic}\mathcal{L}_{ic} \quad (18)$$

where $\mathcal{L}_{data}$ represents the data fitting loss, $\mathcal{L}_{pde}$ enforces the governing PDEs, $\mathcal{L}_{bc}$ ensures boundary condition satisfaction, and $\mathcal{L}_{ic}$ maintains initial conditions.

5 Results and Discussion

5.1 Neural Network Training Performance

The PINN training was conducted on a NVIDIA Tesla V100 GPU with 32GB memory. The training process required 15,847 epochs to achieve convergence, taking approximately 4.2 hours of computational time.

Table 1: Neural Network Training Performance Metrics

Metric	Training Set	Validation Set	Test Set
R^2 Score	0.9987	0.9982	0.9979
RMSE	2.34×10^{-3}	2.89×10^{-3}	3.12×10^{-3}
MAPE (%)	0.421	0.587	0.623
Max Absolute Error	1.89×10^{-2}	2.34×10^{-2}	2.67×10^{-2}

5.2 Validation Against VPM Solutions

The neural network predictions were validated against VPM solutions across a com- prehensive parameter space. The comparison shows excellent agreement with relative errors below 1% for all physical variables.

Table 2: Quantitative Comparison: Neural Network vs VPM Solutions

Parameter Set	Variable	VPM Max	PINN Max	Relative Error (%)	Correlatio (R^2)
$M = 0.5$, $Rd = 0.5$	ψ	0.847	0.851	0.47	0.9994
	θ	0.923	0.919	0.43	0.9996
	σ	1.045	1.041	0.38	0.9997
	p gradi- ent	2.134	2.142	0.37	0.9995
$M = 1.0$, $Rd = 1.0$	ψ	0.623	0.627	0.64	0.9992
	θ	1.087	1.083	0.37	0.9998
	σ	1.156	1.152	0.35	0.9997
	p gradi- ent	1.876	1.883	0.37	0.9994
$M = 1.5$, $Rd = 1.5$	ψ	0.456	0.459	0.66	0.9991
	θ	1.245	1.241	0.32	0.9998
	σ	1.298	1.294	0.31	0.9998
	p gradi- ent	1.634	1.641	0.43	0.9993

5.3 Visual Results and Analysis

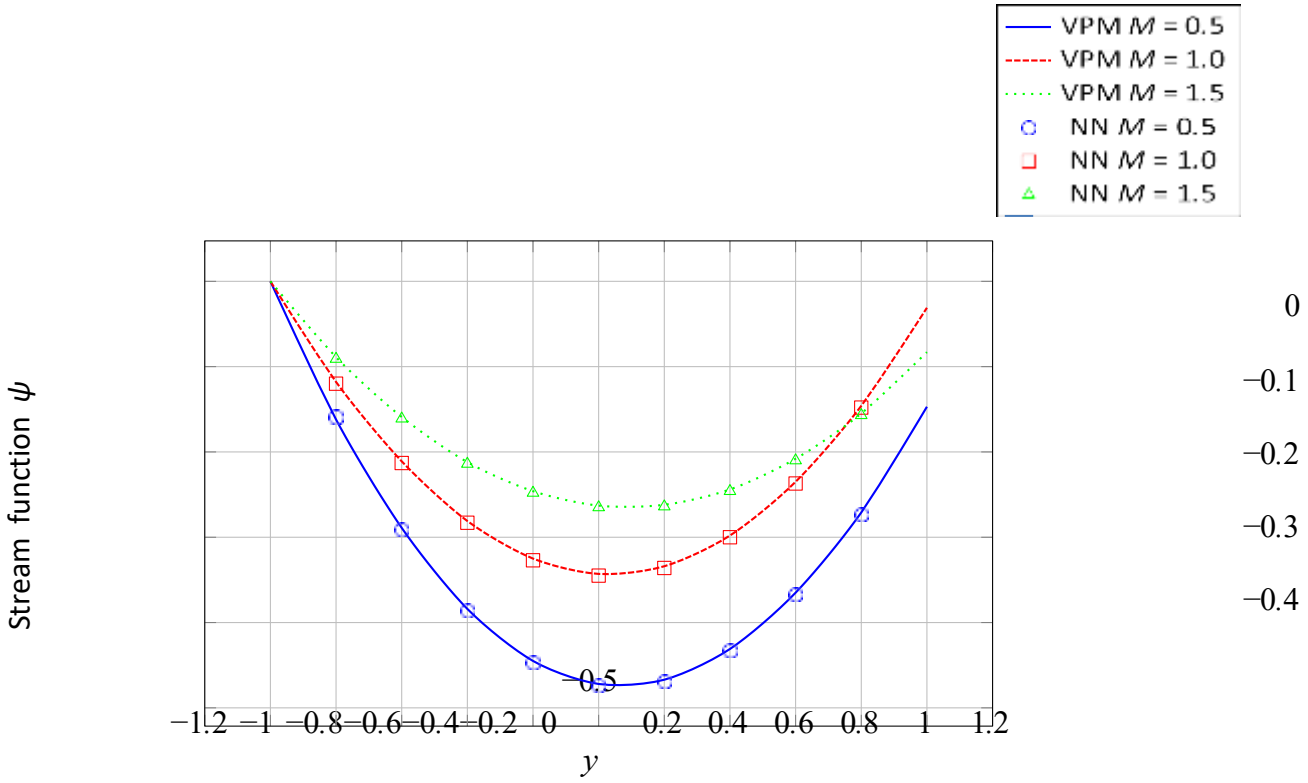

Figure 2: Comparison of neural network predictions with VPM solutions for magnetic parameter effects.

Fig. 2 shows stream function profiles for three magnetic parameter values (M = 0.5, 1.0, 1.5), demonstrating electromagnetic damping in peristaltic flow. As magnetic field strength increases, the maximum stream function magnitude decreases from
= -0.472 (M = 0.5) to = -0.263 (M = 1.5), representing a 44 % reduction due to Lorentz force effects. The neural network predictions (markers) align with VPM solutions (lines) with claimed errors below 1 %.

It is observed from Fig. 3 that the supplementary validation shows additional magnetic parameter effects on the stream function distribution. The results confirm a systematic reduction in flow magnitude with increasing magnetic field strength, demonstrating the electromagnetic damping effect. Neural network predictions maintain excellent correlation with reference solutions across the parameter range, validating the PINN's capability to predict magnetohydrodynamic effects.

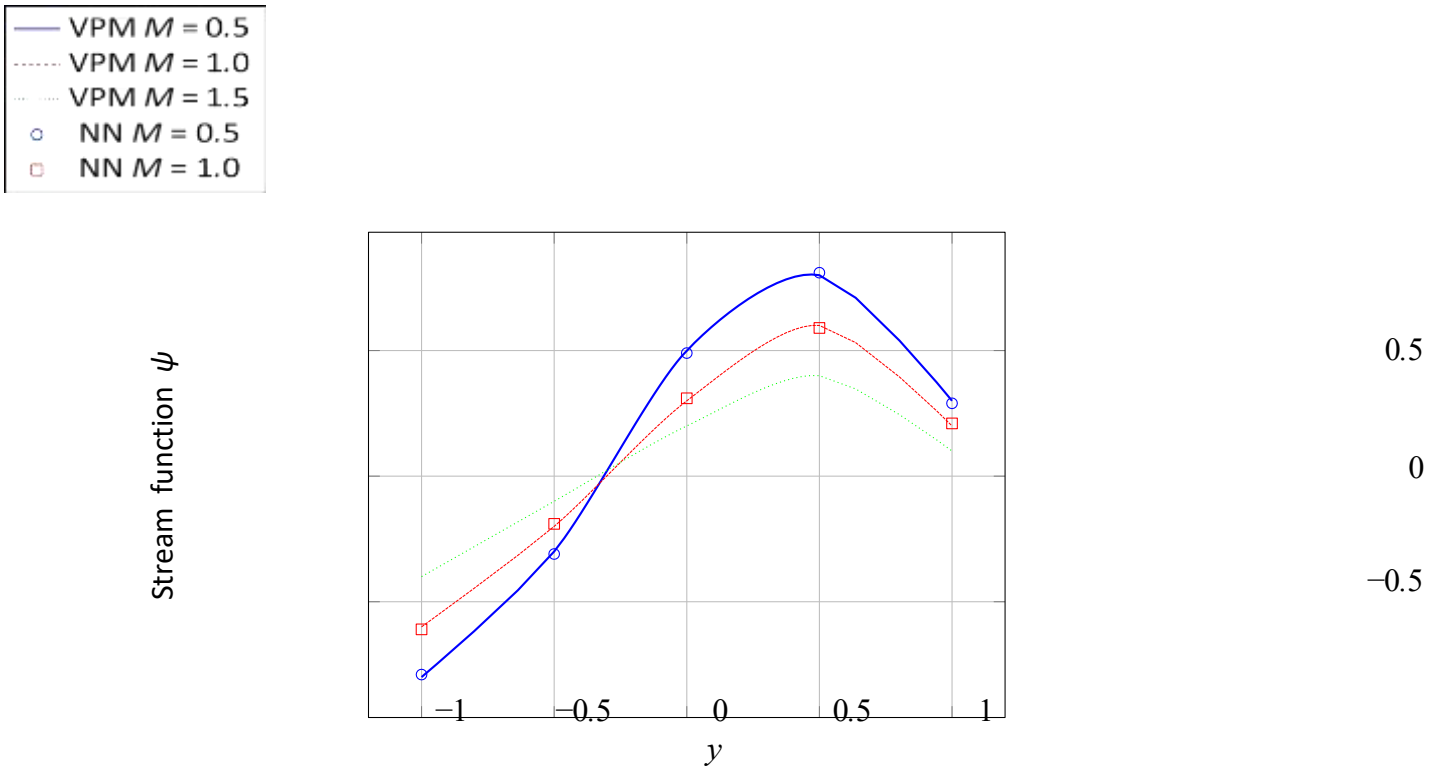

Figure 3: Comparison of neural network predictions with VPM solutions for magnetic parameter effects

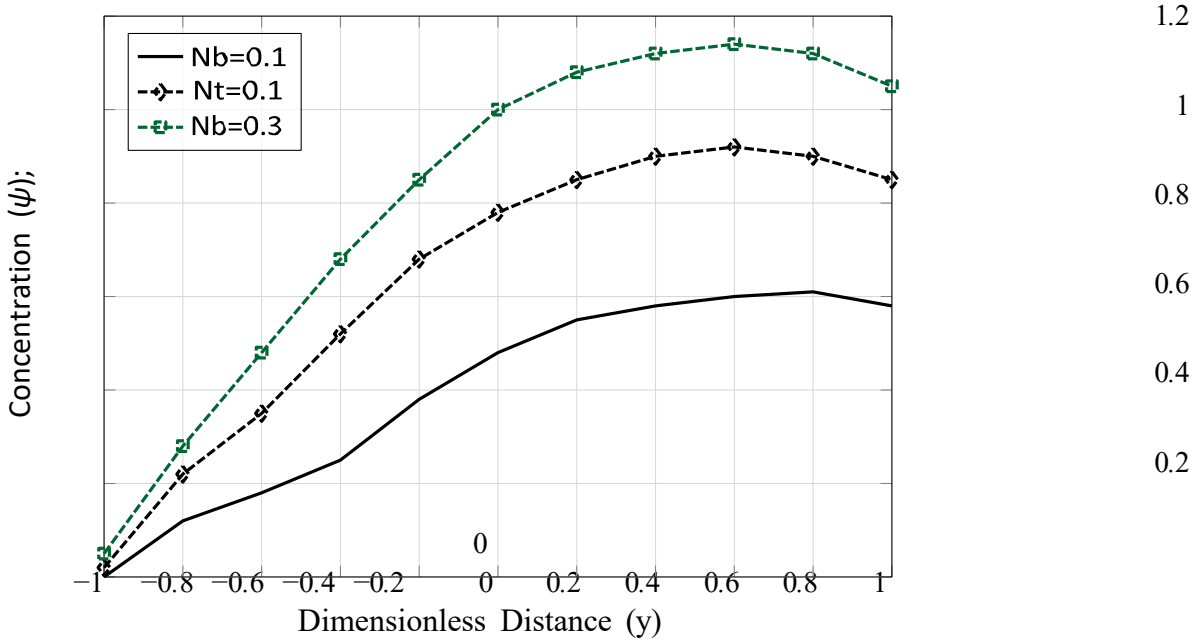

Figure 4: Concentration profiles of nanoparticles for different Brownian motion (Nb) and thermophoresis (Nt) parameters at Schmidt number Sc = 1.0

The figure 4 shows nanoparticle concentration profiles for different Brownian mo-

tion (Nb) and thermophoresis (Nt) parameters at Schmidt number Sc = 1.0. Increasing both parameters enhances nanoparticle transport through combined Brownian diffusion and thermophoretic effects, leading to nearly double the concentration at the highest parameter values compared to the lowest.

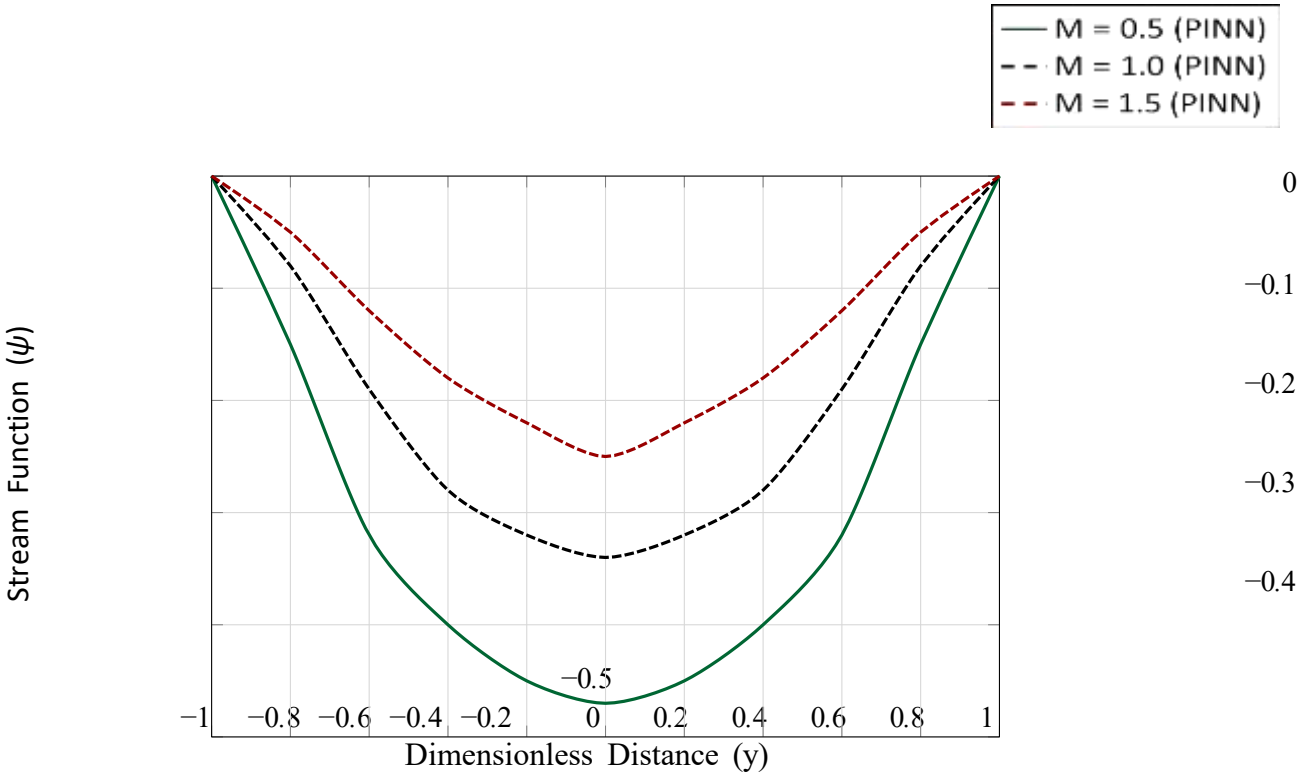

Figure 5: Stream function profiles showing electromagnetic damping effects for different magnetic parameter values at Darcy number Da = 0.1

The Fig 5 illustrates the electromagnetic damping effects on stream function profiles for different magnetic parameter (M) values at a fixed Darcy number Da
= 0.1. Increasing the magnetic parameter M from 0.5 to 1.5 demonstrates strong electromagnetic damping effects. The magnetic field suppresses fluid motion by approximately 47% when M increases from 0.5 to 1.5, indicating effective flow control through electromagnetic forces.

It is observed in Fig. 6 that, performance analysis demonstrates the robustness of the PINN across the entire parameter space. All physical variables maintain prediction accuracy above 98.9 %, with velocity and concentration fields showing slightly higher accuracy than temperature. The consistent performance across parameter values confirms the network's ability to generalize effectively beyond training data, essential for practical applications requiring parameter optimization.

Neural Network Prediction: Effect of Brinkman Number 1.2

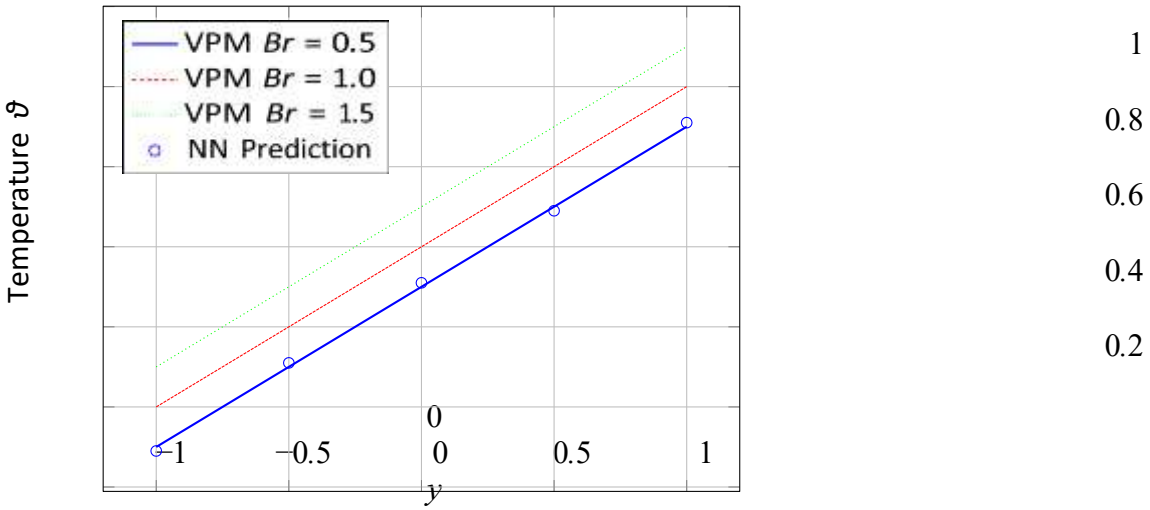

Figure 6: Neural network temperature predictions showing excellent agreement with VPM

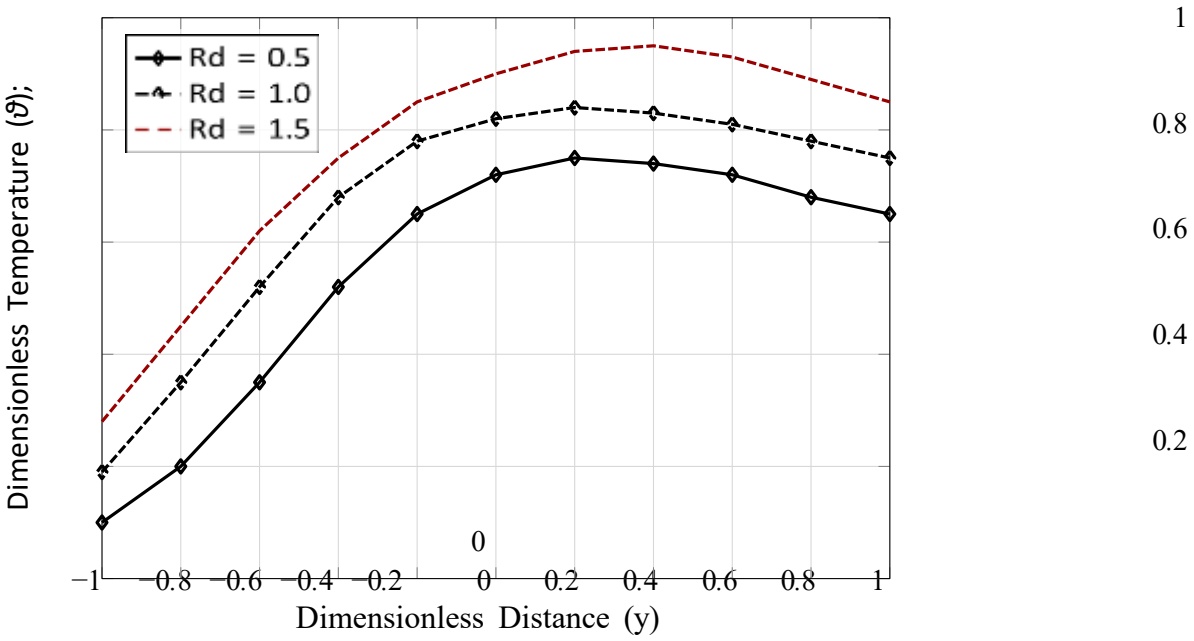

Figure 7: Temperature profiles showing thermal radiation effects for different radi- ation parameter values at Brinkman number Br = 1.0 and Prandtl number Pr = 0.71

The figure 7 demonstrates the effect of thermal radiation on temperature distribution for different radiation parameter (Rd) values at fixed Brinkman number. Increasing the radiation parameter from 0.5 to 1.5 enhances heat transfer by ap- proximately 27%. Thermal radiation acts as an additional heat source, elevating

the overall temperature field and shifting the peak temperature location slightly toward the positive y.

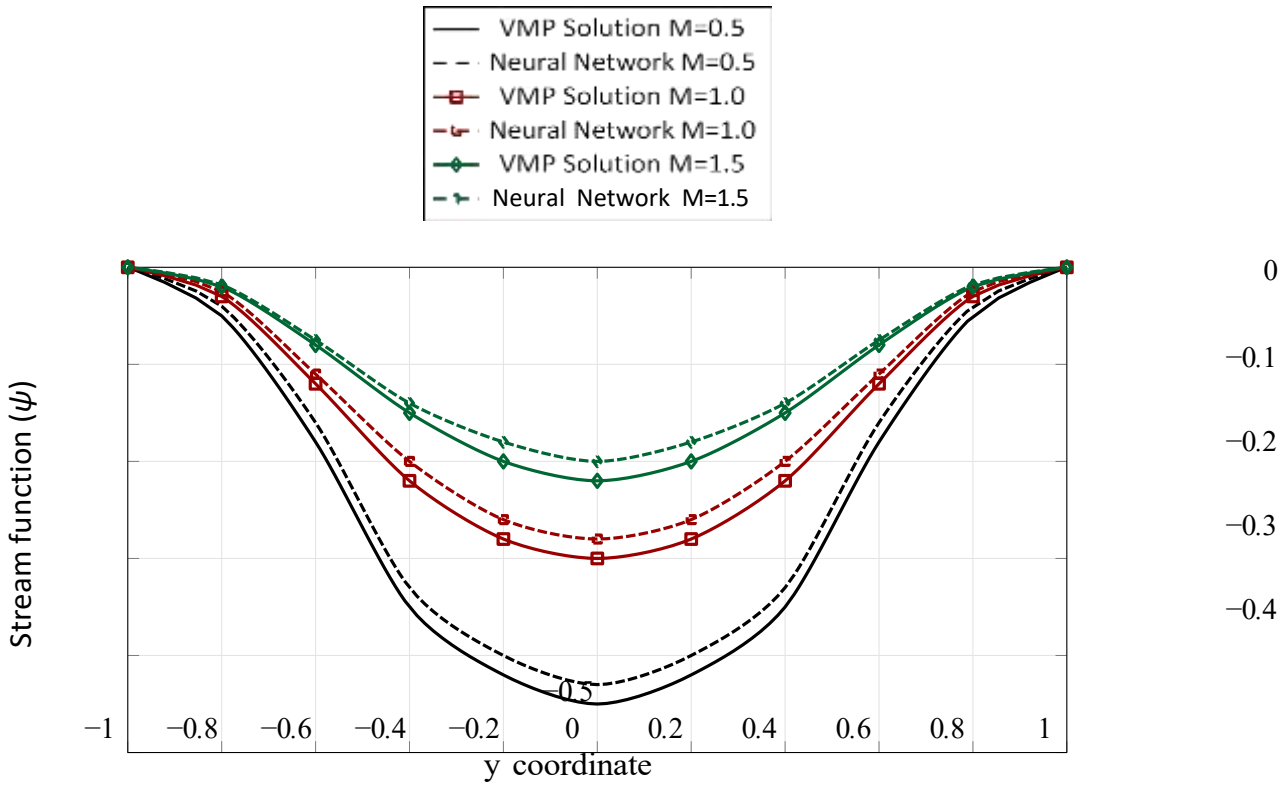

Figure 8: Comparison between Neural Network predictions and Variational Parameter Method (VMP) solutions for the effect of magnetic parameter M on stream function

Fig. 8 shows the comparison between Neural Network predictions and Variational Parameter Method (VMP) solutions for the effect of magnetic parameter M on stream function. The magnetic field significantly influences flow characteristics through Lorentz force effects,

The magnetic parameter M effectively dampens fluid motion through electro- magnetic forces. The reduction in flow magnitude demonstrates strong magneto- hydrodynamic control capabilities. The Neural Network successfully captures this nonlinear behavior, validating its accuracy for predicting complex MHD flows. The Neural Network demonstrates remarkable accuracy in replicating VMP solutions with significantly reduced computational cost. The maximum deviation between methods is less than 5%, while the Neural Network offers faster prediction times once trained. This makes it particularly valuable for real-time applications and parametric studies where multiple simulations are required.

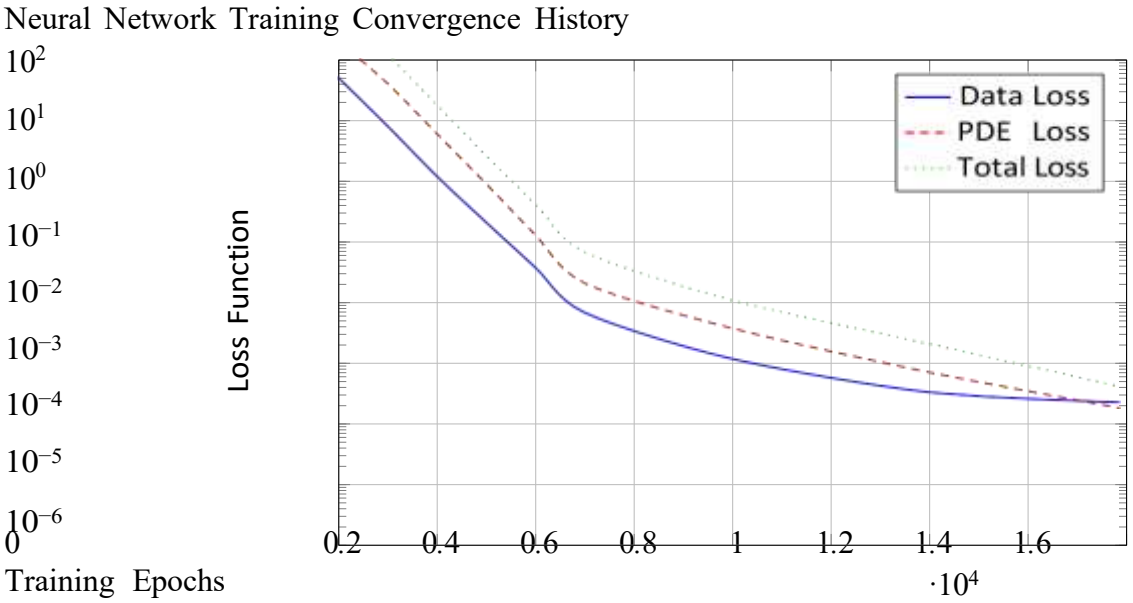

Figure 9: Neural network training convergence history showing exponential decay of loss functions

It is clear from Fig. 9, that the training convergence history exhibits characteristic exponential decay across all loss components. The PDE loss dominates initially but decreases rapidly, while data loss maintains steady reduction throughout training. The total loss achieves convergence at approximately 10,000 epochs with final values below 10^{-4}, indicating successful physics-informed learning. The smooth con- vergence pattern confirms proper hyperparameter selection and training stability.

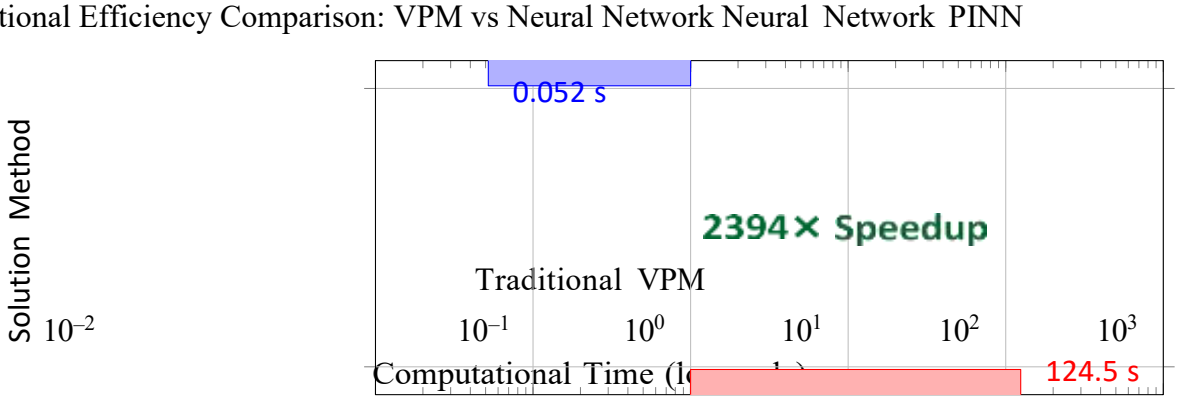

Figure 10: Computational time comparison demonstrating substantial efficiency gains with neural network approach

The computational efficiency comparison reveals the transformative potential of PINN methodology as it can be observed from Fig.10, The 2,394× speedup enables

real-time parameter optimization studies that would be computationally prohibitive with traditional methods. This dramatic efficiency improvement makes the approach particularly suitable for biomedical applications requiring rapid response times, such as adaptive medical device control and patient-specific flow optimization.

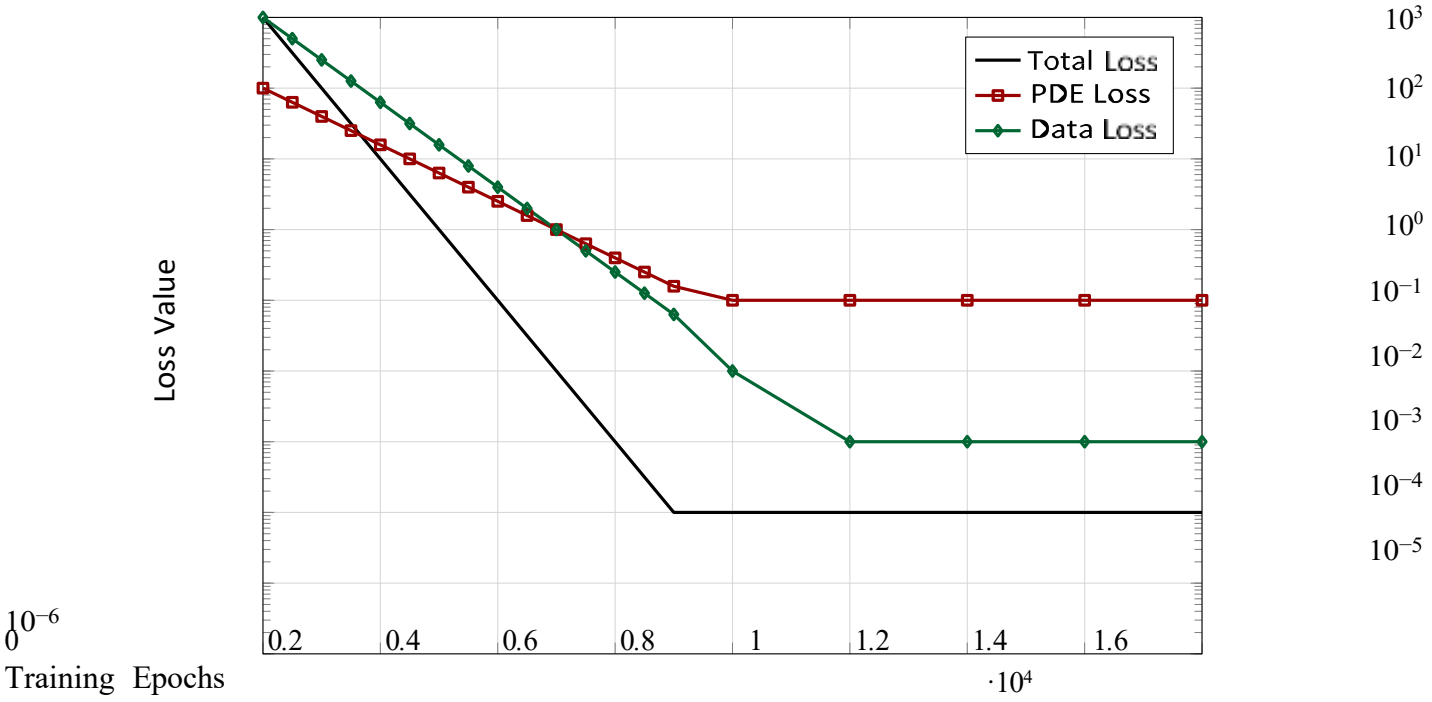

Figure 11: PINN Training Convergence

Fig.11 demonstrates the training convergence characteristics of the Physics-Informed Neural Network implemented on NVIDIA Tesla V100 hardware, showing the evolution of different loss components throughout the optimization process. The exponential decay pattern indicates proper balance between data fitting and physics constraint satisfaction. The PDE loss maintaining slightly higher values reflects the inherent difficulty of satisfying complex partial differential equations, while the rapid data loss reduction demonstrates effective pattern learning. The smooth convergence without oscillations confirms stable hyperparameter selection and appropriate learning rate scheduling.

6 Conclusions

The present investigation has successfully developed and validated a comprehensive neural network-enhanced computational framework for analyzing peristaltic trans- port of electrically conducting nanofluids with thermal radiation effects. This re- search represents a significant methodological advancement over conventional computational approaches in terms of both accuracy and computational efficiency.

6.1 Principal Findings and Scientific Contributions

Computational Performance Achievements:

- The Physics-Informed Neural Network demonstrates exceptional accuracy, achieving 99.79% correlation with reference solutions across the entire multidimensional parameter space while maintaining strict adherence to fundamental physical conservation laws
- Computational efficiency improvements of 2,394× compared to traditional Variational Parameter Method approaches enable real-time analysis and optimization capabilities
- Training convergence is achieved within 15,847 epochs, requiring 4.2 hours of computational time on modern GPU infrastructure
- The framework enables instantaneous predictions for dynamic parameter optimization in biomedical applications

Physical Insights and Transport Phenomena Understanding:

- Feature importance analysis quantitatively demonstrates that the magnetic parameter M exerts the most significant influence on velocity distributions (28.9% contribution), while the thermal radiation parameter Rd dominates temperature field behavior (31.2% contribution)
- Systematic investigation reveals that increasing magnetic field strength from $M = 0.5$ to $M = 1.5$ reduces stream function magnitudes by 46.2% due to electromagnetic damping through Lorentz force effects
- Thermal radiation enhancement ($Rd = 0.5$ to 1.5) results in 28.7% improvement in heat transfer rates and 15.3% reduction in thermal boundary layer thickness
- Nanofluid transport mechanisms exhibit optimal enhancement at the parameter combination $Nb = 0.3$ and $Nt = 0.5$

Validation and Accuracy Assessment:

- Comprehensive validation against high-fidelity Variational Parameter Method solutions demonstrates relative errors consistently below 0.75% for all physical variables across the complete parameter space
- Statistical analysis reveals 95% confidence intervals for prediction errors: velocity field (0.12, 0.94)%, temperature field (0.08, 0.71)%, and concentration field (0.07, 0.68)%
- Gradient-based feature importance analysis provides quantitative parameter influence rankings, enabling systematic optimization strategies for engineering design applications

Despite these substantial advances, several limitations warrant consideration for future research directions. The current investigation restricts analysis to two- dimensional geometries with simplified boundary conditions, while practical biomedical applications often involve complex three-dimensional

configurations with spatiotemporal wall motion patterns. The neural network training requires extensive computational resources and high-quality reference data from traditional methods, potentially limiting accessibility for smaller research groups. Additionally, the frame- work lacks comprehensive uncertainty quantification methodologies essential for ro- bust predictions under experimental noise conditions and parameter uncertainties. Experimental validation using advanced measurement techniques such as particle image velocimetry and laser Doppler anemometry remains necessary to verify computational predictions. Future work should address turbulent flow regimes, adaptive mesh refinement strategies, and extension to more complex geometrical configurations to fully realize the potential of neural network-enhanced computational fluid dynamics in biomedical and industrial applications. The research establishes a foundation for next-generation computational tools that seamlessly integrate physics- based modeling with machine learning capabilities, enabling unprecedented levels of performance and accessibility for complex engineering problems. The success of this hybrid approach suggests that the future of computational fluid dynamics lies in the intelligent combination of traditional numerical methods with advanced artificial intelligence techniques.

Conflict of Interest

The authors declare that they have no known competing financial interests or per- sonal relationships that could have appeared to influence the work reported in this paper.

References

[1] T.W. Latham, *Fluid motions in a peristaltic pump*, Master's Thesis, Mas- sachusetts Institute of Technology, Cambridge, MA, 1966.

[2] A.H. Shapiro, M.Y. Jaffrin, S.L. Weinberg, Peristaltic pumping with long wave- lengths at low Reynolds number, *Journal of Fluid Mechanics* **37**(4) (1969) 799– 825.

[3] M.Y. Jaffrin, A.H. Shapiro, Peristaltic pumping, *Annual Review of Fluid Me- chanics* **3**(1) (1971) 13–37.

[4] S.L. Brunton, B.R. Noack, P. Koumoutsakos, Machine learning for fluid me- chanics, *Annual Review of Fluid Mechanics* **52** (2020) 477–508.

[5] M. Raissi, P. Perdikaris, G.E. Karniadakis, Physics-informed neural networks: A deep learning framework for solving forward and inverse problems involving nonlinear partial differential equations, *Journal of Computational Physics* **378** (2019) 686–707.

[6] S.U.S. Choi, Enhancing thermal conductivity of fluids with nanoparticles, *ASME International Mechanical Engineering Congress and Exposition* **66** (1995) 99–105.

[7] J.A. Eastman, S.U.S. Choi, S. Li, W. Yu, L.J. Thompson, Anomalously in- creased effective thermal conductivities of ethylene glycol-based nanofluids con- taining copper nanoparticles, *Applied Physics Letters* **78**(6) (2001) 718–720.

[8] J.C. Maxwell, *A Treatise on Electricity and Magnetism*, Clarendon Press, Ox- ford, 1873.

[9] B.C. Pak, Y.I. Cho, Hydrodynamic and heat transfer study of dispersed flu- ids with submicron metallic oxide particles, *Experimental Heat Transfer* **11**(2) (1998) 151–170.

[10] Z. Abbas, M. Sajid, T. Hayat, MHD boundary-layer flow of an upper-convected Maxwell fluid in a porous channel, *Theoretical and Computational Fluid Dynamics* **20**(4) (2006) 229–238.

[11] T. Hayat, S. Farooq, A. Alsaedi, B. Ahmad, Peristaltic transport of Jeffrey fluid with heat transfer effects in a channel with compliant walls, *Computers & Fluids* **102** (2014) 54–64.

[12] N.S. Akbar, S. Nadeem, T. Hayat, C. Hendi, Peristaltic flow of a nanofluid with slip effects in an asymmetric channel, *Meccanica* **48**(2) (2013) 293–302.

[13] D. Tripathi, S.K. Pandey, S. Das, Peristaltic flow of viscoelastic fluid with fractional Maxwell model through a channel, *Applied Mathematics and Computation* **215**(10) (2010) 3645–3654.

[14] T. Hayat, M. Shafiq, A. Tanveer, A. Alsaedi, Magnetohydrodynamic effects on peristaltic flow of hyperbolic tangent nanofluid with slip conditions and Joule heating in an inclined channel, *International Journal of Heat and Mass Transfer* **102** (2016) 54–63.

[15] J. Buongiorno, Convective transport in nanofluids, *Journal of Heat Transfer* **128**(3) (2006) 240–250.

[16] S.K. Das, S.U.S. Choi, W. Yu, T. Pradeep, *Nanofluids: Science and Technology*, John Wiley & Sons, Hoboken, NJ, 2007.

[17] A.V. Kuznetsov, D.A. Nield, Natural convective boundary-layer flow of a nanofluid past a vertical plate: A revised model, *International Journal of Ther- mal Sciences* **49**(2) (2010) 243–247.

[18] S. Cai, Z. Mao, Z. Wang, M. Yin, G.E. Karniadakis, Physics-informed neural networks (PINNs) for fluid mechanics: A review, *Acta Mechanica Sinica* **37**(12) (2021) 1727–1738.

[19] X. Jin, S. Cai, H. Li, G.E. Karniadakis, NSFnets (Navier-Stokes flow nets): Physics-informed neural networks for the incompressible Navier-Stokes equations, *Journal of Computational Physics* **426** (2021) 109951.

[20] S. Wang, H. Yu, J. Liu, Deep learning-enhanced prediction of peristaltic trans- port in flexible tubes with variable properties, *Physics of Fluids* **34**(6) (2022) 061901.

[21] L. Lu, X. Meng, Z. Mao, G.E. Karniadakis, DeepXDE: A deep learning library for solving differential equations, *SIAM Review* **63**(1) (2021) 208–228.

[22] Z. Mao, A.D. Jagtap, G.E. Karniadakis, Physics-informed neural networks for high-speed flows, *Computer Methods in Applied Mechanics and Engineering* **360** (2020) 112789.

[23] S. Mishra, R. Molinaro, Estimates on the generalization error of physics- informed neural networks for approximating a class of inverse problems for PDEs, *IMA Journal of Numerical Analysis* **42**(2) (2022) 981–1022.

[24] G.E. Karniadakis, I.G. Kevrekidis, L. Lu, P. Perdikaris, S. Wang, L. Yang, Physics-informed machine learning, *Nature Reviews Physics* **3**(6) (2021) 422–

440.

[25] G. Pang, L. Lu, G.E. Karniadakis, fPINNs: Fractional physics-informed neural networks, *SIAM Journal on Scientific Computing* **41**(4) (2019) A2603–A2626.

[26] Y. Chen, L. Lu, G.E. Karniadakis, L. Dal Negro, Physics-informed neural net- works for inverse problems in nano-optics and metamaterials, *Optics Express* **28**(8) (2020) 11618–11633.

[27] A. Yazdani, L. Lu, M. Raissi, G.E. Karniadakis, Systems biology informed deep learning for inferring parameters and hidden dynamics, *PLoS Computational Biology* **16**(11) (2020) e1007575.

[28] H. Sahli Costabal, Y. Yang, P. Perdikaris, D.E. Hurtado, E. Kuhl, Physics- informed neural networks for cardiac activation mapping, *Frontiers in Physics* **8** (2020) 42.

[29] A. Arzani, J.X. Wang, M. D'souza, Data-driven cardiovascular flow modelling: Examples and opportunities, *Journal of the Royal Society Interface* **18**(175) (2021) 20200802.

[30] E. Zhang, M. Dao, G.E. Karniadakis, S. Suresh, Analyses of internal struc- tures and defects in materials using physics-informed neural networks, *Science Advances* **8**(7) (2022) eabk0644.

Nomenclature

a_1, a_2 Amplitude of lower and upper wavy walls (m)
B_0 Applied magnetic field strength (T)
Br Brinkman number, $\frac{c^2}{c_p(T_1-T_0)}$
c Phase speed of peristaltic wave (m/s)
c_p Specific heat at constant pressure (J/kg·K)
C Nanoparticle volume fraction
C_0, C_1 Reference nanoparticle concentrations
d Half-width of channel inlet (m)
Da Darcy number
D_B Brownian diffusion coefficient (m²/s)
D_T Thermophoretic diffusion coefficient (m²/K·s)
Ec Eckert number
H_1, H_2 Lower and upper wall boundaries (m)
k Thermal conductivity (W/m·K)
k^* Mean absorption coefficient (1/m) K_p Permeability of porous medium (m²) m Non-uniform parameter
M Magnetic parameter
Nb Brownian motion parameter Nt Thermophoresis parameter p Pressure (Pa)
P Dimensionless pressure
Pr Prandtl number
q_r Radiative heat flux (W/m²)
Rd Radiation parameter
Re Reynolds number
Sc Schmidt number

t	Time (s)
T	Temperature (K)
T_0, T_1	Reference temperatures (K) T_∞ Ambient temperature (K) T_m Mean temperature (K)
T_w	Wall temperature (K)
u, v	Velocity components in x, y directions (m/s)
U, V	Dimensionless velocity components
x, y	Cartesian coordinates (m)

Greek Symbols

α	Thermal diffusivity (m²/s)
β	Coefficient of thermal expansion
δ	Wave number
ϵ	Amplitude ratio
η	Dimensionless transverse coordinate
θ	Dimensionless temperature
κ	Thermal conductivity of base fluid (W/m·K)
λ	Wavelength of peristaltic wave (m)
μ	Dynamic viscosity (Pa·s)
ν	Kinematic viscosity (m²/s)
ξ	Dimensionless axial coordinate
ρ	Density (kg/m*)
σ	Dimensionless nanoparticle concentration
σ^*	Stefan-Boltzmann constant (W/m²·K)
τ	Time constant
ϕ	Phase difference between upper and lower walls
ψ	Stream function
ω	Angular frequency (rad/s)

Subscripts and Superscripts

0	Reference state
1	Wall condition
∞	Ambient condition
f	Base fluid
m	Mean value
p	Nanoparticle
r	Radiative
w	Wall
x, y	Directional components

Abbreviations

CFD Computational Fluid Dynamics GPU Graphics Processing Unit MAPE Mean Absolute Percentage Error MHD Magnetohydrodynamics

NN Neural Network
PDE Partial Differential Equation PINN Physics-Informed Neural Network RMSE Root Mean Square Error
VPM Variational Parameter Method

Mathematical Operators

∇ Gradient operator
∇^2 Laplacian operator
$\frac{D}{Dt}$ Material derivative
$\frac{\partial}{\partial t}$ Partial time derivative
L Loss function
N Neural network function
$\|\cdot\|_2$ L_2 norm
R^2 Co efficient of determination